Dynamical Creation of Fractionalized Vortices and Vortex Lattices

An-Chun Ji,[1] W. M. Liu,[1] Jun Liang Song,[2] and Fei Zhou[2]

[1]*Beijing National Laboratory for Condensed Matter Physics, Institute of Physics, Chinese Academy of Sciences, Beijing 100080, China*

[2]*Department of Physics and Astronomy, The University of British Columbia, Vancouver, B. C., Canada V6T1Z1*

(Received 5 February 2008; published 3 July 2008)

We investigate the dynamic creation of fractionalized half-quantum vortices in Bose-Einstein condensates of sodium atoms. Our simulations show that both individual half-quantum vortices and vortex lattices can be created in rotating optical traps when additional pulsed magnetic trapping potentials are applied. We also find that a distinct periodically modulated spin-density-wave spatial structure is always embedded in *square* half-quantum vortex lattices. This structure can be conveniently probed by taking absorption images of ballistically expanding cold atoms in a Stern-Gerlach field.

DOI: 10.1103/PhysRevLett.101.010402 PACS numbers: 03.75.Lm, 03.75.Kk, 03.75.Mn, 67.10.Fj

Topological excitations such as quantized vortices have been fascinating for quite a few decades and recently have also been thoroughly studied in Bose-Einstein condensates (BECs) of ultracold atoms [1–9]. For vortices in single component BECs, the circulation of supercurrent velocity $\mathbf{v}_s$ along a closed curve Γ around a vortex line (defined as $\mathcal{C} = \int_\Gamma d\boldsymbol{l} \cdot \mathbf{v}_s$) is quantized in units of $2\pi\hbar/m$ (m is the atomic mass), with $\mathcal{C} = \pm 1, \pm 2, \ldots$ as a consequence of *analyticity* of single-valued wave functions of coherent quantum states. Furthermore, only a vortex with circulation $\mathcal{C} = \pm 1$ or an elementary vortex is energetically stable. A secondary vortex with circulation $\mathcal{C} = \pm 2, \pm 3, \ldots$ spontaneously splits into a few elementary ones which interact via long range repulsive potentials.

A configuration with its circulation smaller than the elementary value ($\mathcal{C} = 1$) has to be described by a singular wave function and it always turns out to be energetically catastrophic. A most obvious example is a two-dimensional configuration, where the condensate phase angle $\Phi(r, \theta)$ rotates slowly and uniformly by 180° in the $r - \theta$ plane around a vortex center but jumps from π to 2π when the polar angle θ is equal to 2π. The π-phase jump here effectively induces a singular *cut* in the wave-function. The corresponding circulating velocity field is simply $\mathbf{v}_s(r, \theta) = \hbar/(2mr)\mathbf{e}_\theta$, leading to $\mathcal{C} = 1/2$ that is one-half of an elementary value. The energy of a *cut* per unit length along $\theta = 2\pi$ line where the phase jumps is finite and therefore the overall energy of a *cut* in an individual fractionalized-vortex scales as L, L is the size of system, while the energy for an integer vortex only scales as a logarithmic function of L. Consequently, a *cut* that connects two singular fractionalized vortices mediates a linear long rang *attractive* potential that confines all fractionalized excitations. So in a single component condensate, vortices with $\mathcal{C} = \pm 1$ are fundamental ones which do not further split into smaller constituent elements as a result of confinement of fractionalized vortices.

Hyperfine-spin degrees of freedom can drastically change the above arguments about elementary vortices. In condensates of sodium (^{23}Na) or rubidium (^{87}Rb) atoms in optical traps [10], hyperfine spins of cold atoms are correlated because of condensation. A *pure* spin defect (or a spin disclination in the case of ^{23}Na) where spins of cold atoms slowly rotate but no supercurrents flow, can carry a *cut*, i.e., a line along which a π-phase jump occurs as a result of Berry's phases induced by spin rotations [11]. Such a spin defect can then terminate a *cut* emitted from a singular half-quantum vortex (HQV) configuration, which consequently leads to a linear confining potential between the spin defect and HQV. For instance, a HQV with $\mathcal{C} = 1/2$ confined to a spin defect does exist as a fundamental excitation in spin nematic condensates [12,13]. In this Letter we will present the simulation of dynamical creation of fractionalized HQVs in a rotating BEC of sodium atoms, and formulate an experimental procedure for the realization of such exotic topological excitations.

Magnetic properties and energetics of half vortices.— Unlike conventional integer vortices, HQVs have very rich magnetic structures. We will demonstrate that far away from its core a HQV have vanishing local spin densities but is accompanied by slowly rotating spin quadrupole moments; within the core, spin densities are nonzero. The Hamiltonian for interacting sodium atoms is

$$H = \int d\mathbf{r}\psi_\alpha^\dagger(\mathbf{r})\frac{-\hbar^2\nabla^2}{2m}\psi_\alpha(\mathbf{r}) + \frac{c_2}{2}\int d\mathbf{r}\hat{\mathbf{S}}^2(\mathbf{r}) + \frac{c_0}{2} \times \int d\mathbf{r}\hat{\rho}^2(\mathbf{r}). \quad (1)$$

Here $\psi_\alpha^\dagger(\psi_\alpha)$, $\alpha = x, y, z$ are creation (annihilation) operators for sodium atoms in hyperfine states $|\alpha\rangle$; they are defined as linear superpositions of creation operators for three spin-one states, $|1, m_F\rangle$, $m_F = 0, \pm 1$. $\psi_x^\dagger = (\psi_1^\dagger - \psi_{-1}^\dagger)/\sqrt{2}$, $\psi_y^\dagger = (\psi_1^\dagger + \psi_{-1}^\dagger)/i\sqrt{2}$ and $\psi_z^\dagger = \psi_0^\dagger$. $c_{0,2}$ are interaction parameters that depend on two-body s-wave scattering lengths $a_{0,2}$ for total spin 0, 2: $c_0 = 4\pi\hbar^2(a_0 + 2a_2)/3m$ and $c_2 = 4\pi\hbar^2(a_2 - a_0)/3m$. For condensates of ^{23}Na atoms, $a_0 \simeq 50a_B$ and $a_2 \simeq 55a_B$ (a_B is the Bohr

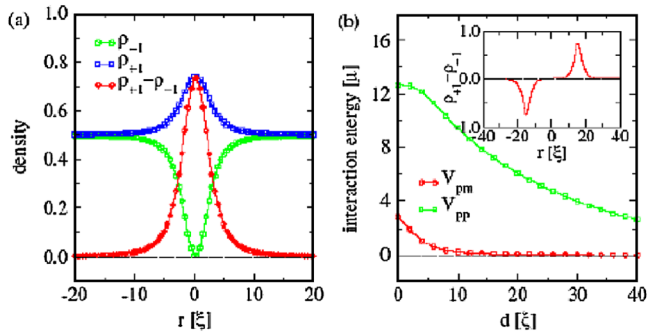

FIG. 1 (color online). (a) Density ($\rho_{\pm 1} = |\psi_{\pm 1}|^2$) and spin-density ($\rho_1 - \rho_{-1}$) profiles of an individual *plus* half-quantum vortex (HQV) centered at $r = 0$. (b) Interaction potentials (in units of chemical potential μ) between two HQVs as a function of separation distance d. V_{pm} is the potential between a plus HQV and a minus HQV; V_{pp} is the strong repulsive potential between two *plus* HQVs. Inset is for spin densities in a pair of plus-minus HQVs separated at $d = 30\xi$, ξ is the healing length.

radius). $\hat{\mathbf{S}}_\alpha = -i\epsilon_{\alpha\beta\gamma}\Psi^*_\beta\Psi_\gamma$ and $\hat{\rho} = \psi^\dagger_\alpha\psi_\alpha$ are local spin-density and density operators.

Generally, a condensate wave function $\Psi_\alpha(= \langle\psi^\dagger_\alpha\rangle)$ for spin-one atoms is a complex vector. For sodium atoms, interactions favor states with a zero spin density; this leads to a spin nematic ground state which does not break the time reversal symmetry and $\Psi = \exp(i\Phi)\sqrt{\rho}\mathbf{n}$; here $\mathbf{n}$ is a unit vector with three components n_α, and ρ is the number density of sodium atoms. This spin nematic state is invariant under an inversion of $\mathbf{n}$ and a π-phase shift (i.e., $\mathbf{n} \rightarrow -\mathbf{n}$ and $\Phi \rightarrow \Phi + \pi$). Although local spin densities $\langle\hat{\mathbf{S}}(\mathbf{r})\rangle$ in a nematic state vanish, a nematic condensate carries a spin quadrupole moment defined as $Q_{\alpha\beta}(\mathbf{r}) = \langle\hat{\mathbf{S}}_\alpha\hat{\mathbf{S}}_\beta\rangle - \frac{1}{3}\delta_{\alpha\beta}\langle\hat{\mathbf{S}}^2\rangle$, which can be calculated and is specified by the nematic unit director $\mathbf{n}$ introduced above: $Q_{\alpha\beta} = \rho(\mathbf{n}_\alpha\mathbf{n}_\beta - \frac{1}{3}\delta_{\alpha\beta})$.

Around a HQV centered at the origin and oriented along the z direction, nematic directors lying in a perpendicular $r - \theta$ plane rotate by 180° forming a spin-disclination; the corresponding condensate wave function far way from the vortex core is $\Psi(\theta, r \rightarrow \infty) = \exp(i\theta/2)\sqrt{\rho}\mathbf{n}(\theta)$, $n_x = \cos(\theta/2)$, $n_y = \sin(\theta/2)$ and $n_z = 0$. The 180° rotation of nematic director $\mathbf{n}(\theta)$ around the vortex illustrates that a π-spin disclination where spin quadrupole moments $Q_{\alpha\beta}(\theta)$ slowly rotate is indeed confined to this HQV. In the Zeeman basis of $|1, m_F\rangle$ states, $m_F = 0, \pm 1$, the above vortex state is equivalent to $\psi_1 = \exp(i\theta)f(r)\sqrt{\rho}/\sqrt{2}$, $\psi_{-1} = -g(r)\sqrt{\rho}/\sqrt{2}$ and $\psi_0 = 0$; far away from the vortex core, $f(r \rightarrow \infty) = g(r \rightarrow \infty) = 1$. The core structure can be studied by numerically solving the multiple-component Gross-Pitaevskii (GP) equation

$$\left[-\frac{\hbar^2}{2m}\nabla^2 + (c_0 + c_2)\rho_{\pm 1} + (c_0 - c_2)\rho_{\mp 1}\right]\psi_{\pm 1} = 0, \tag{2}$$

here $\rho_{m_F} = |\psi_{m_F}|^2$. The corresponding boundary conditions when $r \rightarrow \infty$ are set by the asymptotic behaviors of a HQV far away from the core as discussed before Eq. (2). Notice that the last term in Eq. (2) indicates that mutual interactions between $|1, \pm 1\rangle$ atoms induced by scattering are repulsive since $c_0 - c_2$ is positive.

Our results show that within the core, $|1, 1\rangle$ atoms state are completely depleted while $|1, -1\rangle$ atoms are not. This is because supercurrents are only present in the $|1, 1\rangle$ component; in fact the density of $|1, -1\rangle$ atoms has an additional small bump at the center of core, to further take advantage of the depletion of $|1, 1\rangle$ atoms in the same region to minimize the overall repulsive interactions between $|1, \pm 1\rangle$ atoms. So the core has a nonzero local spin density $\langle\hat{\mathbf{S}}_z(\mathbf{r})\rangle(= |\psi_1|^2 - |\psi_{-1}|^2)$ with excess atoms at $|1, -1\rangle$ state and we define it as a *minus* HQV. Similarly, one can construct a *plus* HQV with an identical vorticity (i.e., $\nabla \times \mathbf{v}_s$) but with excess $|1, 1\rangle$ atoms in its core [see Fig. 1(a)]. Generally, HQVs have distinct spatial magnetic structures: a HQV core carries excess spins while far away from the core spin quadrupole moments slowly rotate around the vortex.

Interactions between two HQVs very much depend on species of HQVs involved. When both are *plus* ones (or *minus*), the corresponding interaction potential $V_{pp(mm)}$ is a logarithmic long range one due to interference between coherent supercurrents. However, the interaction between a *plus* and a *minus* HQV V_{pm} is repulsive and short ranged only extending over a scale of vortex cores. In this case, supercurrents flow in different components and they do not interfere; the short range interaction is entirely due to intercomponent interactions between $|1, 1\rangle$ and $|1, -1\rangle$ atoms. Indeed, the amplitude of potential V_{pm} is proportional to, when it is small, $c_0 - c_2$ which characterizes mutual interactions between $|1, \pm 1\rangle$ atoms. An integer vortex or a pair of *plus-minus* HQVs centered at a same point therefore is unstable and further fractionalizes into elementary HQVs. In Fig. 1, we summarize results of an individual HQV and two HQVs.

Dynamical creation of HQVs in rotating BECs.—To dynamically create HQVs, we numerically solve the time-dependent coupled GP equations of spin-1 BEC

$$\begin{aligned}(i - \gamma)\hbar\frac{\partial\psi_{\pm 1}}{\partial t} &= \Big[-\frac{\hbar^2}{2m}\nabla^2 + V_{\mathrm{tr}} - \mu \mp \lambda - \Omega L_z \\ &\quad + c_0\rho + c_2(\rho_{\pm 1} + \rho_0 - \rho_{\mp 1}) \\ &\quad + W_\pm\Big]\psi_{\pm 1} + c_2\psi_0^2\bar{\psi}_{\mp 1}, \\ (i - \gamma)\hbar\frac{\partial\psi_0}{\partial t} &= \Big[-\frac{\hbar^2}{2m}\nabla^2 + V_{\mathrm{tr}} - \mu - \Omega L_z + c_0\rho \\ &\quad + c_2(\rho_1 + \rho_{-1})\Big]\psi_0 + 2c_2\psi_1\psi_{-1}\bar{\psi}_0,\end{aligned} \tag{3}$$

where $\rho = \sum_{m_F}\rho_{m_F}$ is the total condensate density, $V_{\mathrm{tr}}(\mathbf{r})$

is a spin-independent confining potential of an optical trap, and $W_{\pm}(\mathbf{r})$ are pulsed magnetic trapping potentials which we further apply in order to create HQVs. μ and λ are the Lagrange multipliers used to preserve the total number and magnetization of atoms respectively; γ is a phenomenological damping parameter which is necessary for studies of quasistationary states [7].

We restrict ourselves to a cigar-shaped potential with the aspect ratio $\lambda = \omega_\perp/\omega_z \sim 14$ which was also used in early experiments [2]. We consider a two-dimensional cylindrical trap which is characterized by two dimensionless parameters $C_0 = \frac{8\pi N(a_0+2a_2)}{3L_z}$ and $C_2 = \frac{8\pi N(a_2-a_0)}{3L_z}$, with L_z the size of system along the z axis and $N = 3 \times 10^6$ the total number of sodium atoms. When combined with a nonaxisymmetric dipole potential that can be created using stirring laser beams [2,4], the optical trapping potential in a *rotating frame* is given by $V_{\mathrm{tr}}(\mathbf{r}) = m\omega_\perp^2\{(1+\epsilon)x^2 + (1-\epsilon)y^2\}/2$. Here $\omega_\perp = 2\pi \times 250$ Hz, and anisotropic parameter is set to be $\epsilon = 0.025$. We also include an additional magnetic trapping potential: $W_{\pm}(\mathbf{r}) = \mp\beta m\omega_\perp^2(x^2+y^2)/2$, which could be realized in an Ioffe-Pritchard trap via a Zeeman splitting $m_F g_F \mu_B B$ with the Landé factor $g_F = -1$ for sodium atoms.

We start our numerical simulations with an initial state where $|1, \pm 1\rangle$ are equally populated. Experimentally, it was demonstrated that when the bias field is small and the gradient field along the z axis of the trap is almost canceled, such a state can be prepared and the $|1, \pm 1\rangle$ components are completely miscible (however, with the immiscibility between $|1, \pm 1\rangle$ and $|1, 0\rangle$ components) [10]. We then study the time evolution of this initial state using the Crank-Nicolson implicit scheme [7]. The unit of length is $a_h = \sqrt{\hbar/2m\omega_\perp} = 0.48$ μm and the period of the trap is $\omega_\perp^{-1} = 4$ ms; the interaction parameters are $C_0 = 500$ and $C_2 = 450$ and the damping rate is $\gamma = 0.03$. Further, we include symmetry breaking effects in our simulations by allowing the trap center to randomly jump within a region $[-\delta, \delta] \times [-\delta, \delta]$ ($\delta = 0.001h$, where h is the grid size), which is crucial for vortices to enter the condensate one by one [9] rather than in opposing pairs [7,8].

However, without additional pulsed magnetic potentials, one can show that dynamic instabilities for creation of integer vortices in rotating BECs occur almost at same frequencies as for HQVs and a triangular integer-vortex lattice is formed [see Fig. 3(a)]. This integer-vortex lattice is locally stable with respect to the nonmagnetic perturbations, by applying an additional optical trapping potential with an oscillating trapping frequency to effectively *shake* them, indicating their metastability. For this reason, a time-dependent magnetic trapping potential with harmonic form is applied, and we find that when a pulsed magnetic field with $\beta > 0.005$ is applied, HQV lattices could be formed. Here we set $\beta = 0.1$, which is suitable for both generating a single HQV and demonstrating the dynamical evolution of HQV lattices formation. After the magnetic trapping potentials are on, $|1, 1\rangle$ component further spreads to the edge, while $|1, -1\rangle$ component remains at the center of the trap and surfaces of equally populated $|1, \pm 1\rangle$ components become mismatched with two different Thomas-Fermi radii.

First, we dynamically create a single half-quantum vortex in condensates, which can be used for the study of dynamics of a HQV. We switch on abruptly a rotating drive with $\Omega = 0.65\omega_\perp$ and the trap anisotropy ϵ is increased rapidly from zero to its final value 0.025 in 20 ms. At $t =$ 800 ms, only one vortex in $|1, -1\rangle$ component appears. Afterwards, We decrease Ω to $0.3\omega_\perp$ suddenly, and switch off the magnetic trapping potential adiabatically within 200 ms. We then find a stable single HQV formed at $t =$ 1600 ms as shown in Fig. 2. The $0.3\omega_\perp$ frequency used after $t = 1600$ ms is within the stable region estimated earlier [14] and our simulations of dynamics are consistent with the energetic analysis.

Fractionalized-vortex lattices can be created in a similar setup. The main experimental procedure and results of our simulations for creation of HQV lattices are presented in Fig. 3. After a rotation with frequency $\Omega = 0.7\omega_\perp$ starts abruptly and anisotropy ϵ is set to its final value 0.025, we can see that the cloud is initially elongated and at the same time rotates with the trap. At about 150 ms, surface ripples due to quadrupole excitations occur in $|1, 1\rangle$ component of the condensate, while no surface oscillations appear on the surface of $|1, -1\rangle$ component. At $t = 240$ ms, we find that the density profile of $|1, 1\rangle$ component is along a short-axis while the $|1, -1\rangle$ component is along a long-axis due to repulsive interactions between two components, and the surface of $|1, -1\rangle$ component is not always buried in the inner region of $|1, 1\rangle$. The surfaces of two components oscillate independently and are decoupled dynamically. At $t = 430$ ms, we find that two *plus* HQVs with excess $|1, 1\rangle$ atoms inside cores have nucleated at the center. Correspondingly, we observe two small regions near the center where $|1, -1\rangle$ atoms are completely depleted and the density of $|1, 1\rangle$ atoms remains high. At $t = 800$ ms,

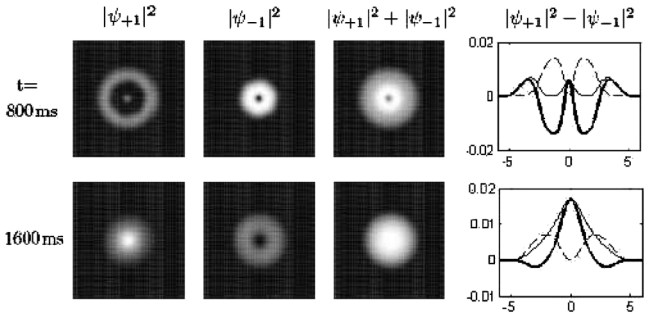

FIG. 2. Creation of a half-quantum vortex. Density profiles of $|\psi_{+1}|^2$, $|\psi_{-1}|^2$, $|\psi_{+1}|^2 + |\psi_{-1}|^2$, and spin-density profile $|\psi_{+1}|^2 - |\psi_{-1}|^2$ (bold line) are shown. The rotating frequency is suddenly decreased from an initial value $\Omega = 0.65\omega_\perp$ to $\Omega = 0.3\omega_\perp$ at $t = 800$ ms. The bottom panel shows that a single half-quantum vortex is formed at $t = 1600$ ms after the magnetic trapping potential has been adiabatically switched off.

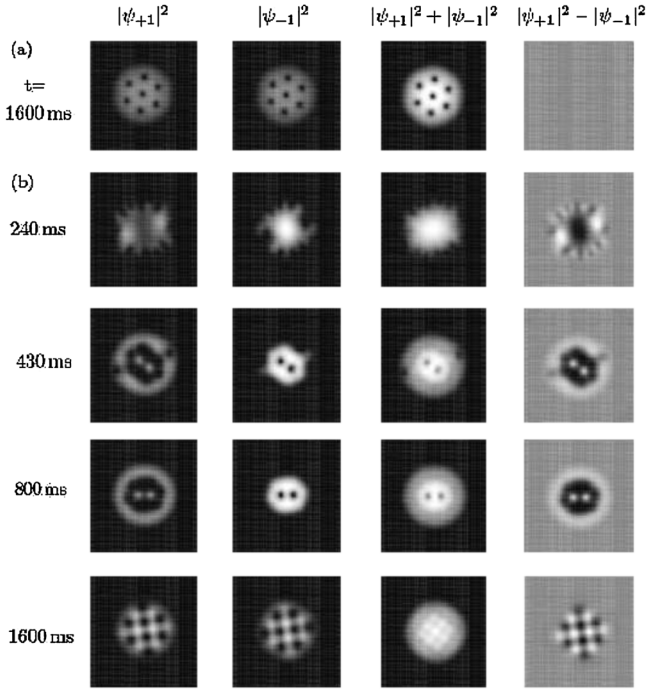

FIG. 3. (a) Creation of a triangular integer-vortex lattice in a rotating optical trap at $t = 1600$ ms. (b) Creation of half-quantum vortex lattices when an additional pulsed magnetic trapping potential is applied. Here time evolution of various condensate densities is shown. The optical trap rotates at $\Omega = 0.7\omega_\perp$ with a magnetic trapping potential on until $t = 800$ ms; afterwards, the magnetic trap is adiabatically switched off within 200 ms. The bottom panel shows the half-quantum vortex lattice formation at $t = 1600$ ms; a square lattice in the spin-density profile is clearly visible.

two components are phase separated, but the structure of HQV cores remains almost unchanged. Finally, we switch off the additional magnetic potential adiabatically within 200 ms and a HQV lattice with interlaced square configuration becomes visible. In this structure, to minimize strong repulsive interactions $V_{pp(mm)}$ between *plus* or *minus* HQVs, the vorticity is evenly distributed among plus and minus HQVs, or between $|1, \pm 1\rangle$ components. This also indicates that spatially each plus HQV prefers to be adjacent to minus HQVs and *vice versa* to avoid stronger interactions V_{pp}, V_{mm} and to take advantage of relative weaker interactions V_{pm} (See Fig. 1). To further minimize repulsive interactions V_{pm} between nearest neighboring vortices, a *plus* HQV is displaced away from adjacent minus HQVs by a maximal distance. Generally, because of the asymmetry between V_{pp} and V_{pm}, a bipartite vortex lattice should be favored over frustrated geometries such as triangular lattices where a plus HQV could be adjacent to another plus HQV resulting in much stronger repulsion. In our simulations of ^{23}Na atoms in rotating traps with $c_0 \simeq 30c_2$, square vortex lattices have always been found. Equilibrium energetics of rectangular or square lattices were also considered in the quantum Hall regime [15,16], in two-component BECs coupled by an external driving field where vortex molecules are formed [17], and also observed in condensates of pseudo-spin-1/2 rubidium atoms [18]. Here we have mainly focused on *dynamical creation* of HQV lattices confined to a spin-density-wave structure at relatively low frequencies; this structure can be conveniently probed by taking absorption images of ballistically expanding cold atoms in a Stern-Gerlach field [10].

In conclusion, we have demonstrated a practical setup to create fractionalized vortices and vortex lattices in BECs of sodium atoms. We found that a *square* half-quantum vortex lattice has a distinct periodically modulated spin-density-wave spatial structure, due to short range repulsive interactions between neighboring half-quantum vortices. Our results are of particular significance for creating these excitations in experiments and for exploring novel phenomena associated with them.

F. Z. would like to thank E. Demler, W. Ketterle, K. Madison for stimulating discussions. This work is supported by the office of the Dean of Science, UBC, NSERC (Canada), Canadian Institute for Advanced Research, A. P. Sloan foundation; NSFC under Grants No. 90406017, No. 60525417, and the NKBRSFC under Grant No. 2006CB921400.

[1] M. R. Matthews *et al.*, Phys. Rev. Lett. **83**, 2498 (1999); J. E. Williams and M. J. Holland, Nature (London) **401**, 568 (1999).
[2] K. W. Madison *et al.*, Phys. Rev. Lett. **84**, 806 (2000); K. W. Madison *et al.*, Phys. Rev. Lett. **86**, 4443 (2001).
[3] P. C. Haljan *et al.*, Phys. Rev. Lett. **87**, 210403 (2001).
[4] J. R. Abo-Shaeer *et al.*, Science **292**, 476 (2001).
[5] A. L. Fetter *et al.*, J. Phys. Condens. Matter **13**, R135 (2001); D. L. Feder *et al.*, Phys. Rev. Lett. **86**, 564 (2001).
[6] F. Dalfovo and S. Stringari, Phys. Rev. A **63**, 011601 (2000).
[7] M. Tsubota *et al.*, Phys. Rev. A **65**, 023603 (2002).
[8] E. Lundh *et al.*, Phys. Rev. A **67**, 063604 (2003).
[9] N. G. Parker *et al.*, Phys. Rev. Lett. **95**, 145301 (2005).
[10] J. Stenger *et al.*, Nature (London) **396**, 345 (1998).
[11] D. J. Thouless, *Topological Quantum Numbers in Nonrelativistic Physics* (World Scientific, Singapore, 1998).
[12] F. Zhou, Phys. Rev. Lett. **87**, 080401 (2001).
[13] U. Leonhardt and G. E. Volovik, JETP Lett. **72**, 46 (2000).
[14] T. Isoshima and K. Machida, Phys. Rev. A **66**, 023602 (2002); T. Isoshima *et al.*, J. Phys. Soc. Jpn. **70**, 1604 (2001).
[15] T. Kita *et al.*, Phys. Rev. A **66**, 061601 (2002).
[16] E. J. Mueller and T. L. Ho, Phys. Rev. Lett. **88**, 180403 (2002).
[17] K. Kasamatsu *et al.*, Phys. Rev. Lett. **91**, 150406 (2003).
[18] V. Schweikhard *et al.*, Phys. Rev. Lett. **93**, 210403 (2004).